Co-published by
Institute of Fluid-Flow Machinery
Polish Academy of Sciences
Committee on Thermodynamics and Combustion
Polish Academy of Sciences

http://www.imp.gda.pl/archives-of-thermodynamics/

ARCHIVES OF THERMODYNAMICS

Thermodynamic modelling of a power generation plant using solar concentrators assisted by organic Rankine cycle for João Pessoa city, Brazil

Taynara G. S. Lago[a*], Beatriz R. P. Padilha[b], Felipe S. Teixeira[a], João A. Lima[a]
Adriano S. Marques[a] and Carlos M. S. Santos[c]

[a]Department of Renewable Energy Engineering, Centre of Renewable and Alternative Energy, Federal University of Paraíba, João Pessoa – PB, Brazil
[b]Postgraduate Program in Energy Planning, Faculty of Mechanical Engineering, State University of Campinas, Campinas – SP, Brazil.
[c]Centre for Exact and Technological Sciences, Federal University of Recôncavo da Bahia, Cruz das Almas –BA, Brazil.
*Corresponding author email: taynara@cear.ufpb.br

Received: 10.07.2024; revised: 02.10.2024; accepted: 11.10.2024

Abstract

The potential for generating electricity through solar energy makes Brazil a very promising country in this segment, with several possibilities for the use of solar energy, whether in the thermal or photovoltaic part, due to the high incidence of solar radiation throughout much of the country, especially in the Northeast region. In this study, an analysis of the performance of the organic Rankine cycle (ORC) that produces electricity using solar concentrators was performed. The fluids used in the system were classified as dry type – toluene, isobutane, isopentane, R227ea, R113, R114, R245fa and R600. During the study, the energy and exergy analysis of the system was conducted for different evaporator pressures (500−2500 kPa), and two types of solar collectors were tested (parabolic trough collector and parabolic compound collector). In addition, a system case study was simulated for radiation and temperature conditions in the city of João Pessoa, Brazil. Based on this analysis, the performance of the cycle components was examined, and the first and second law efficiencies of the system were compared for different configurations. The solar collector (parabolic trough collector) proved to be the most suitable for the studied cycle. With the adequate selection of the refrigerant, collector and evaporation pressure, the first and second law efficiencies of the cycle improve up to 41% and 44%, respectively. For the city of João Pessoa, the highest exergy efficiency occurs in the month of January, the hottest month of the year when the sun shines brightly, and the lowest exergy efficiency occurs in the month of June.

Keywords: Organic Rankine cycle; Renewable energy; Concentrated solar power; Thermal and exergetic analysis

Vol. 46(2025), No. 1, 123–134; doi: 10.24425/ather.2025.154187

Cite this manuscript as: Lago, T.G.S., Padilha, B.R.P., Teixeira, F.S., Lima, J.A., Marques, A.S., & Santos, C.M.S. (2025). Thermodynamic modelling of a power generation plant using solar concentrators assisted by organic Rankine cycle for João Pessoa city, Brazil. *Archives of Thermodynamics*, 46(1), 123–134.

1. Introduction

Thermodynamic modelling of organic Rankine cycles (OCRs) has been the subject of increasing interest in the fields of engineering. These cycles, based on the principle of the classic Rankine cycle, are fundamental for the efficient generation of energy from renewable and sustainable sources. Unlike conventional cycles that use water as the working fluid, organic Rankine cycles employ organic compounds with low boiling points as working fluids, enabling the utilization of low-temperature heat sources such as waste heat from industrial processes or solar energy. The increasing interest in renewable and environmentally friendly sources of energy has driven research and development efforts towards power generation systems based on this technology.

Nomenclature

a_1, a_2, a_3 – heat loss coefficients, 1/K, W/(m^2 K), W/(m^2 K^2)
A – area, m^2
C_p – specific heat at constant pressure, kJ/(kg K)
DNI – direct normal irradiance, W/m^2
Ex – exergy, kW
h – specific enthalpy, kJ/kg
Δh – enthalpy change, kJ/kg
$\dot{m}$ – mass flow rate, kg/s
P – pressure, kPa
$\dot{Q}$ – heat transfer rate, kJ/kg
s – entropy, kJ/(kg K)
T – temperature, K
v – specific volume, m^3/kg
w – work, kJ/kg
$\dot{W}$ – power, kW

Greek symbols

ε – effectiveness of the heat exchanger
η – efficiency
ψ – exergy, kJ/kg

Subscripts and Superscripts

a – solar collector aperture
amb – ambient
b – pump
collector – solar collector
con – condensation
condenser – condenser
evaporator – evaporator
f, fluid – fluid
i – point in the cycle
in, out – inlet, outlet
liq – liquid
o – dead-state conditions
Pump,isen – isentropic pump process
rad – radiation
regenerator – regenerator
sun – surface of the sun
t – turbine
ther – overall thermal
Turbine,isen – isentropic turbine process
$II, Collector$ – second law of the collector
$II, Condenser$ – second law of the condenser
$II, Evaporator$ – second law of the evaporator
$II, Regenerator$ – second law of the regenerator
$II, Turbine$ – second law of the turbine

Abbreviations and Acronyms

CPC – compound parabolic collector
FPC – flat plate solar collector
HTF – heat transfer fluid
ORC – organic Rankine cycle
PTC – parabolic trough collector

Colonna et al. [1] provided a bibliographic review, illustrating the concept of organic Rankine cycles, emphasizing that these cycle technologies offer flexibility in terms of capacity and temperature for thermal energy conversion applications. The authors highlight that these systems have broad applications in cogeneration systems, involving both heating and cooling, as well as thermal energy distribution systems. In this study, the fundamental elements of the thermodynamic cycle, such as the working fluid, design aspects, and the advantages and disadvantages in comparison to other technologies, are detailed.

According to Loni et al. [2], the relationship between solar irradiation and the use of solar thermal energy combined with thermodynamic cycles is a promising technology due to the high compatibility between the operating temperature of the collectors and the temperature required for the cycle to function, meeting the minimum conditions to achieve viable efficiency. In this perspective, research and development efforts in the context of using it as a secondary source of energy employ these solar collector systems in subprocesses of the cycles, such as enhancing boiler heating.

Petrollese et al. [3] investigated the solar energy concentrate ion plant (CSP) with an organic Rankine cycle integrated into the Ottana solar facility as a means of concentrating solar technologies for power supply. In this case, the thermal plant consists of a CSP unit (630 kW) with thermal storage coupled to a 400 kW concentrated photovoltaic plant with electrochemical storage, acting to promote planned energy profiles for the succeeding day based on meteorological data and weather forecasts. Regarding the CSP plant, it was determined that the ORC performance is inherently related to the thermal oil operational profiles, inlet temperature, and ambient temperature. Therefore, the researchers emphasized the significant importance of the daily start-up and shut-down phases of the ORC unit to enhance the overall plant performance.

Ancona et al. [4] conducted an analysis of a prototype of an organic Rankine cycle coupled to a commercial model of a solar collector, aiming to reduce the annual costs of electricity for a household. Initially, the collector surface and the tank were sized to simulate the performance of organic fluids and low-global warming potential mixtures. Results show that the system with R134a can cover approximately 39% of the yearly electricity demand, corresponding to more than 1150 kWh.

An optimization analysis of the low-temperature solar organic Rankine cycle was conducted by Delgado-Torres and García-Rodríguez [5]. The study involved examining twelve potential working fluids for ORC and four stationary solar collector models to determine the most efficient system with the minimum required area. One viable application observed by the authors is the integration of the organic Rankine cycle with solar thermal energy and the low-energy consumption desalination technology, reverse osmosis. Jing et al. [6] developed a mathematical model to optimize a system of low temperature solar thermal electric generation based on compound parabolic concentrators (CPC) and an organic Rankine cycle working with HCFC-123, and evaluated its annual performance in different areas of Canberra, Singapore, Bombay, Lhasa, Sacramento and Berlin. Kumar and Shukla [7] investigated the application of benzene as the working fluid for the ORC system to assess the performance of the organic Rankine cycle. The thermal solar plant modelled for this study features a binary cycle, where the first cycle operates with the heat transfer fluid in a liquid state, and the second cycle operates with the organic fluid, benzene. To analyse the efficiency behaviour, output powers of 8 kW, 9 kW, and 10 kW were applied. The best result was obtained at the 9 kW power level, where the ORC system efficiency ranged from 32.87% to 54.98%, with the turbine outlet temperature varying from 259.53°C to 127.22°C.

Sonsaree et al. [8] proposed a model for a small-scale solar organic Rankine cycle power plant in Thailand with R-245af, operating with a compound parabolic concentrator, evacuated-tube or flat-plate collectors as the devices for generating heat. The maximum power output, the CO_2 emission, and the economic analysis in terms of the levelised cost of electricity were analysed. Stand et al. [9] proposed in their study an idea for a hybrid solar-biomass system for electricity generation in remote areas in Colombia. In this case, the hybridization integrates the supercritical Brayton cycle (SBC) and organic Rankine cycle, a solar field composed of concentrated solar tower technology, and coconut shell biomass. For the elaboration of this work, energy and exergy analysis were necessary for the following scenarios: solar-biomass hybrid SBC-ORC, SBC-ORC/Solar, and SBC-ORC/Biomass. The study concluded that the solar-biomass hybrid system SBC-ORC presented the best exergetic efficiency among the three cases, thus showing the possibility of implementing this project. Additionally, they also highlighted the coconut shell's high calorific value and the dissemination of its energetic use to contribute to the socioeconomic development of the agricultural sector in Colombia.

Gupta et al. [10] reviewed the main thermodynamic methods applied in organic Rankine cycles, with the authors' primary focus being on the issue of multi-utilization of ORC to couple concentrated solar collectors with an environmentally viable biomass system, where ORC would supply more than one type of energy, i.e. applied in the context of thermal and electrical energy conversion.

The storage system in thermal solar energy projects is essential for utilizing electrical energy during periods of reduced solar irradiation. Therefore, based on this scenario, Lakhani et al. [11] developed a dynamic model applied to the thermal energy storage system using latent heat in solar thermal power plants with an organic Rankine cycle. The mentioned energy storage system consists of a shell-and-tube heat exchanger where the phase change material is stored on the shell side, while the heat transfer fluid (HTF) flows through the tubes. Through this mechanism, HTF can meet the plant's nighttime demand during moments when the organic fluid cannot reach the saturation temperature.

Li et al. [12] performed an experimental study on a parabolic trough concentrated solar ORC system by using nitrate salt as the heat transfer and storage medium, and a single screw expander for power conversion. They carried out energy and exergy analyses of the overall system evaluating the dynamic changes in the temperature of PTC, molten salt tank and ORC. It was observed that the collector efficiency, expander efficiency and ORC efficiency were relatively lower than the published data. In accordance with Ahmadi et al. [13], organic Rankine cycles originating from a geothermal source can be technically viable, favouring the substitution of conventional fossil energy sources. The choice of a hybrid system that operates under favourable low-temperature conditions, such as geothermal energy (below 150°C), enables a systematic approach in which the authors emphasize the economic aspect of the ORC's efficiency applied in this context.

The nanofluid acting as the working fluid has a long history of experiments and scientific foundation that enabled the manufacturing of specific thermodynamic components for this type of fluid. Therefore, Saadatfar et al. [14], through a modelling program, designed the thermodynamic cycle to produce energy, heating and cooling using an organic Rankine cycle with nanofluid as the working fluid. This research involved a comparison between an organic nanofluid and a base fluid, namely silver nano pentane and pure pentane, respectively. The established analysis concluded that the best cycle efficiency results were found for the organic nanofluid, requiring smaller heat exchangers and expanders.

More recently, Rejeb et al. [15] developed a 3E mathematical model (energy, exergy and economic) to simulate and optimize a poligeneration system (H_2, O_2, electricity and heat production) consisting of solar photovoltaic thermal collectors with organic Rankine cycle, proton exchange membrane (PEM) electrolyser and liquefied natural gas. They used the non-dominated sorting genetic algorithm II (NSGA-II) to estimate the optimal results for the proposed system with the energy efficiency, cost rate and net output power as the objective functions.

Youtao et al. [16] evaluated a direct vapour generation for a solar organic Rankine cycle (DVG-ORC) system under different operating conditions. The results show that the evaporation temperature has different impacts on the system performance. R245ca and R1336mzz(Z) exhibit a higher net output power at different evaporation temperatures, with R1336mzz(Z) only reducing it by 3.73–5.26% compared to R245ca. In addition, R1336mzz(Z), of low global warming potential (GWP), demonstrates the highest system efficiency, making it the most suitable working fluid for the DVG-ORC system due to its environmental friendliness and safety.

Maytorena and Buentello-Montoya [17] simulated a parabolic trough collector system filled with benzene under solar irradiation for use in an organic Rankine cycle. Different inlet temperatures (465, 475 and 485 K), mass fluxes (168, 336 and 504 kg/(m^{2}s)), and solar-concentrated heat fluxes (15.1, 18.5 and 22.2 kW/m^2) are used in the simulations. The results indicate that increasing the mass flow rate decreases the fluid evaporation rate, the fluid evaporation rate is directly affected by the solar heat flux and the mass flux affects the point where evaporation begins (tube lengths of 10, 15 and 25 m for mass fluxes of 168, 336 and 504 kg/(m^{2}s), to 15.1 kW/m^2, respectively).

Based on recent literature, this article aims to explore the thermodynamic modelling of these innovative cycles, highlighting their benefits, challenges and potential applications. It also aims to encourage studies related to the search for more sustainable fluids, collaborating to intensify the research and development of ORC plants applied to solar thermal systems in the context of electric generation. Its main contribution is a study of the potential of a solar power generation plant using the organic Rankine cycle in a city in the northeast region of Brazil, the city of João Pessoa (never studied), through an energy and exergy analysis with different fluids and solar concentrators in a simple plant without storage, which can be applied by entrepreneurs in the region and reproduced by other researchers for mapping resources in other regions.

2. Method and materials

Figure 1 shows a methodological routine flowchart of the study. The methodological procedures applied in the work were based on mathematical modelling and simulation of a traditional conventional regenerative Rankine cycle scheme with the coupling of solar concentrators as a heat source. The input data are cycle parameters, concentrator characteristics, type of fluids and solar irradiance. With this data, an energetic and exergy analysis is made. The efficiency results are reported as a function of the evaporation temperature.

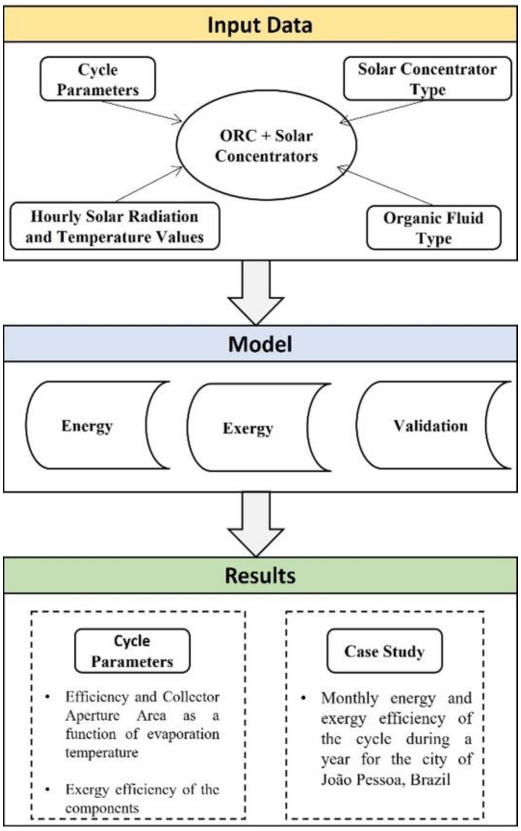

Fig. 1. Flowchart of methodology used in the research.

2.1. Cycle studied

Figure 2 shows the typical low-temperature organic Rankine cycle configuration with solar concentrators in the heat supply function as the hot source for system operation. The processes in Fig. 2 are:

- Process 1–2: The working fluid enters the pump as a saturated liquid and leaves under pressure as a subcooled liquid. There is no heat transfer during the process.
- Process 2–3: With the compression of the liquid performed by the pump, the compressed fluid is slightly heated in the regenerator using the saturated vapour that leaves the turbine.
- Process 3–4: Heat is supplied to the compressed liquid in the evaporator due to heat exchange with the fluid from the solar field. The temperature of the organic Rankine fluid increases at constant pressure, passing the fluid to a superheated state.
- Process 4–5: After the expansion of the fluid performed by the turbine, there is a decrease in the temperature and pressure properties until it enters the regenerator.
- Process 5–6: Saturated vapour passes through the regenerator to heat the compressed fluid.
- Process 6–1: Heat rejection in the condenser. The saturated vapour becomes saturated liquid.
- Process 7–8: Solar field fluid is pumped to the solar concentrator.
- Process 8–9: Solar fluid is heated in a solar concentrator.
- Process 9–7: Solar fluid supplying heat to organic fluid in the evaporator.

This type of configuration is not only applicable to solar collectors but also in other applications, such as in geothermal energy systems, due to its simplicity and low cost.

The system was mathematically modelled in the software EES – Engineering Equation Solver. To develop the model, the mass and energy balance equations were adopted for control volumes in a steady state regime, with negligible kinetic and potential energy variations and flow without a pressure drop. The equations and conditions adopted are described in the following sections.

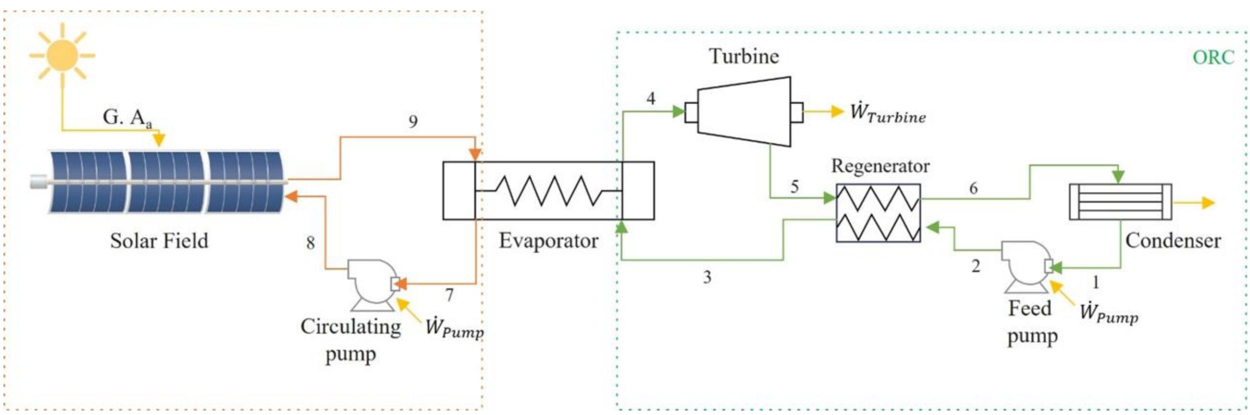

Fig. 2. Organic Rankine cycle with solar concentrators.

2.2. The energy analysis of the cycle studied

An energy analysis is performed for the studied cycle, through the equation of the first law of thermodynamics applied to all cycle components. The energy equations of the cycle components are described as follows:

Figure 3 shows the control volume in the turbine. In this equipment, work is produced, so the energy balance is described by

$$\dot{W}_{Turbine} = \dot{m}(h_4 - h_5). \tag{1}$$

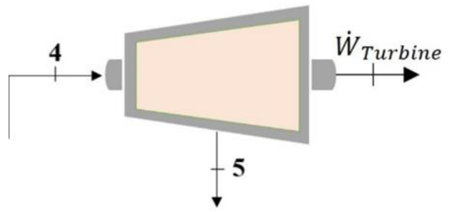

Fig. 3. Turbine control volume.

Through the isentropic efficiency of the turbine, it is possible to determine the real work between 4 and 5 and the enthalpy at the output, according to the following equation:

$$\eta_{Turbine,isen} = \frac{h_4 - h_5}{h_4 - h_{5s}}. \tag{2}$$

Figure 4 shows the control volume in the condenser. In this heat exchanger, the heat exchange between 6 and 1 is given by the following equation:

$$\dot{Q}_{condenser} = \dot{m}(h_6 - h_1). \tag{3}$$

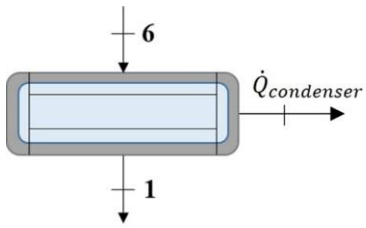

Fig. 4. Condenser control volume.

Figure 5 shows the volume control in the pump. The pump fluid is an incompressible fluid, i.e., $v_1 = v_2$, so the pump work between 1 and 2 is given by the following equations:

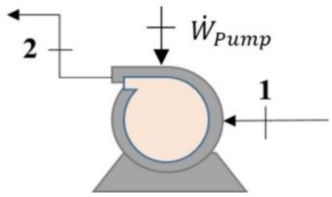

Fig. 5. Pump control volume

$$-w_{Pump} = \int v dP \cong v_1(P_2 - P_1) = h_{2s} - h_1, \tag{4}$$

$$h_{2s} = h_1 + v_1(P_2 - P_1). \tag{5}$$

Through the isentropic efficiency of the pump, it is possible to determine the real work between 1 and 2 and the enthalpy at the output, according to the following equation:

$$\eta_{Pump,isen} = \frac{h_{2s} - h_1}{h_2 - h_1}. \tag{6}$$

Figure 6 shows the control volume in the regenerator. The heat transfer in the regenerator is calculated by the following equation:

$$\dot{Q}_{regenerator} = \varepsilon \dot{m} C_p (T_5 - T_2). \tag{7}$$

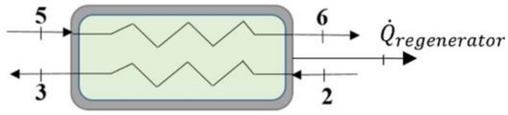

Fig. 6. Regenerator control volume.

Figure 7 shows the control volume in the evaporator. The heat transfer in the evaporator is calculated by the following Eqs. (8)–(13):

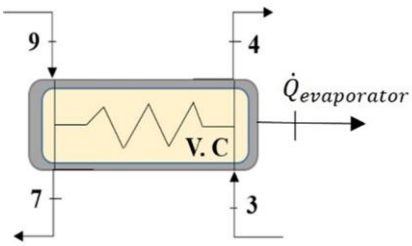

Fig. 7. Evaporator control volume.

$$\dot{Q}_{evaporator} = \dot{m}(h_4 - h_3), \tag{8}$$

$$\eta_{\mathrm{ORC}} = \frac{\dot{W}_{liq}}{\dot{Q}_{evap}} = 1 - \frac{\dot{Q}_{condenser}}{\dot{Q}_{evaporator}}, \tag{9}$$

$$\eta_{ther} = \eta_{\mathrm{ORC}} \cdot \eta_{collector}, \tag{10}$$

$$A_a = \frac{\dot{Q}_{evaporator}}{\mathrm{DNI} \cdot \eta_{collector}}, \tag{11}$$

$$\eta_{ther} = \frac{\dot{W}_{liq}}{\mathrm{DNI} \cdot A_a}. \tag{12}$$

Considering that there are no heat losses to the surroundings in the evaporator between the ORC and the solar collector circuit and taking into account the definition of the collector efficiency and the overall efficiency of the solar ORC in the configuration with heat transfer fluid, the thermal efficiency is given by

$$\eta_{ther} = \frac{\dot{W}_{liq}}{\mathrm{DNI} \cdot A_a} = \eta_{collector}\left[\eta_{\mathrm{ORC}} + \frac{\Delta h_{\mathrm{HTF},7 \to in(8)}(\eta_{\mathrm{ORC}} - 1)}{\Delta h_{\mathrm{HTF},in(8) \to out(9)}}\right]. \tag{13}$$

2.3. The exergy analysis of the organic Rankine cycle

Exergy is a thermodynamic property that defines the maximum theoretical work that can be obtained as the reference environment interacts to equilibrium with the system of interest. Therefore, T_o represents the dead-state temperature for exergy calculations, h_o and s_o stand for the enthalpy and entropy of the operating fluid in the dead-state conditions (at the pressure and temperature), respectively. Additionally, h_i and s_i represent enthalpy and entropy for each point in the cycle. Using these variables, exergy ψ_i is determined for each point in the cycle according to the following equation:

$$\psi_i = h_i - h_o - T_o(s_i - s_o). \tag{14}$$

The second-law efficiency of various devices with steady-state flow can be determined based on its general definition, which is the ratio of the recovered exergy to the supplied exergy. The second-law efficiencies of the turbine, condenser, evaporator, and regenerator can be defined through Eqs. (15)–(18), respectively:

$$\eta_{II,Turbine} = \frac{\dot{W}_{liq}}{(\psi_4 - \psi_5)}, \tag{15}$$

$$\eta_{II,Condenser} = 1 - \left[\frac{T_O(s_6 - s_1) + \frac{\dot{Q}_{condenser}}{T_{con}}}{\dot{m}(\psi_6 - \psi_1)}\right], \tag{16}$$

$$\eta_{II,Evaporator} = \frac{\dot{m}_{fluid}(\psi_4 - \psi_3)}{\dot{m}_{\mathrm{HTF}}(\psi_9 - \psi_7)}, \tag{17}$$

$$\eta_{II,Regenerator} = \frac{\dot{m}_{fluid}(\psi_3 - \psi_2)}{\dot{m}_{\mathrm{HTF}}(\psi_5 - \psi_6)}. \tag{18}$$

The exergetic efficiency, or the second law of a coupled system, can help reduce irreversibility in the system and increase the efficiency of thermal processes. The increased efficiency, in turn, reduces the energy required by the systems, given that the expression for the exergetic efficiency can be defined by (Hepbasli [18])

$$\eta_{II,Collector} = \frac{\dot{m}_{\mathrm{HTF}}(\psi_9 - \psi_8)}{\mathrm{Ex}_{rad}}. \tag{19}$$

The exergy of solar radiation was calculated using the Petela equation presented in Eq. (20) (Hepbasli [18]):

$$\mathrm{Ex}_{rad} = A_a \cdot \mathrm{DNI} \cdot \left[1 + \frac{1}{3}\left(\frac{T_O}{T_{sun}}\right)^4 - \frac{4}{3}\frac{T_O}{T_{sun}}\right]. \tag{20}$$

The term within parentheses has a value of 0.934 for the surface temperature of the sun at 6000 K and an ambient temperature of 298 K.

2.4. Refrigerant fluid selection

Due to the huge variety of working fluids available for use in organic Rankine cycles, it was necessary to carry out the selection of representative fluids for computer simulation. The criteria for the selection were:

- Critical temperature higher than the minimum study temperature;
- Dry fluids, i.e. $\theta < 87°$ (θ is the angle of inclination of the tangent line to the saturated vapour curve (dT/ds), humid $\theta > 93°$; isentropic fluids $\theta \cong 90°$, evaluated at the saturation temperature for 80% of the critical pressure);
- Give preference to hydrocarbons, as they have a simpler molecular structure and lower cost;
- Search for fluids of distinct thermodynamic properties to enrich comparisons;
- Toxicity category A by the American Society of Heating, Refrigerating and Air-Conditioning Engineers (ASHRAE).
- Fluids used in the literature, to verify their efficiency, since they have already been selected for this purpose in other studies.

Applying the criteria described above, a shortlist of 8 potential fluids was arrived at for study: toluene, isobutane, isopentane, R227ea, R113, R114, R245fa, R600.

Table 1. Solar collectors and operating temperature range.

Type of Collector	Operating Range (°C)
Flat plate collector	80–100
Evacuated tube collector	80–160
Compound parabolic collector	120–170
Parabolic trough collector	170–300

2.5. Solar collectors

Table 1 shows collectors for heating water or producing energy and their operating temperature range (Nafey and Sharaf [19]).

Given various types of solar collectors, three types of collectors are most studied: flat plate collector (FPC), parabolic trough collector (PTC) and compound parabolic collector (CPC). Linear Fresnel reflectors and solar towers have the characteristic of having their performance determined by the geometry of the solar field and the arrangement of the individual mirrors, and there is no efficiency equation independent of the geometric configuration. The efficiency equations for parabolic, evacuated tube, flat plate and compound parabolic collectors are easier to find in the literature.

Among the collectors with an experimentally determined efficiency curve, only the parabolic trough and compound parabolic trough collectors are widely used for power production. These choices are related to the temperature range linked to the efficiency of these two collectors for concentration systems, since they are the main collectors used in this type of application (Kalougirou [20]). For this reason, these two classes of collectors were simulated, according to Eq. (21) and Table 2:

$$\eta_{collector} = \eta_0 - a_1(\bar{T}_f - T_{amb}) - \frac{a_2(\bar{T}_f - T_{amb})}{\mathrm{DNI}} - \frac{a_3(\bar{T}_f - T_{amb})^2}{\mathrm{DNI}}. \tag{21}$$

Table 2. Parameters of solar collectors.

Type	Collector	η_0	a_1	a_2	a_3
PTC	EuroTrough	0.750	0.039	0.0003	0.000045
CPC	CPC Aosol 1.12X^2	0.736	4.610	0.0000	0.000000

This collector efficiency is related to the efficiency of zero loss (η_0), heat loss coefficients with temperature (a_1, a_2, a_3), and finally, the technical parameters of irradiance on the collector (DNI) and the average temperatures of the fluid flowing inside the collector ($\overline{T_f}$) and the surroundings (T_{amb}).

2.5. Validation

To ensure the accuracy of the thermodynamic model developed within the scope of this study and the reliability of the obtained results, this model must be validated by studies in the literature. In order to verify the developed model, the organic Rankine cycle was simulated in a manner analogous to the work of Delgado-Torres and García-Rodríguez [5] comparing collector efficiency parameters, ORC efficiency and overall efficiency (thermodynamic and solar cycle). The calculated parameters included the heat supplied by the system, i.e. by the solar concentrators, the rejected heat, as well as the work of the pumps and turbines, which were already considered in a situation close to reality, without assuming compression and expansion as isentropic.

Table 3 reports the results found by the thermodynamic simulation of the organic Rankine cycle in comparison with the results of Delgado-Torres and García-Rodríguez [5]. With the consolidated program in EES, different configurations were investigated for the solar ORC cycle. Table 3 shows the parameters considered in the simulation.

Table 3. Input parameters for the proposed simulation.

Fluids of the Organic Rankine Cycle	**Isobutane; Isopentane; Toluene; R245fa**
Isentropic efficiency of the turbine (η_t)	0.75
Isentropic efficiency of the pump (η_b)	0.80
Effectiveness of the regenerator (ε)	0.80
Evaporation pressure	500–2500 kPa
Working fluid in the collector	Terminol-VP1
Ambient temperature (T_{amb})	25°C
Condensation temperature (T_{cond})	25°C;
Average irradiance on the collector (DNI)	1000 W/m²
Net power generated	1 kW
Solar collectors used	FPC; PTC; CPC

For the simulated cycle, the Terminol-VP1 fluid was chosen due to its suitability for use in solar concentrating systems. It was also verified that it meets the desired temperature requirement, remaining non-flammable within the temperature and pressure range used in the simulation proposed by this study. Furthermore, to gather information regarding the average fluid temperature in the collector ($\overline{T_f}$), temperatures of 300°C were assumed for the parabolic trough collector, 170°C for the compound parabolic collector, and 100°C for the flat plate solar collector, in a non-concentrated configuration, to obtain results with a high level of reliability for this temperature range applied to both collectors [20]. The pumping power of the heat transfer fluid was neglected.

The System Advisor Model (SAM) software was used to study the direct normal irradiation of the location of CEAR – Center for Alternative and Renewable Energy. The representative average days of each month were chosen according to those recommended by Klein [21]. The average values for direct solar radiation corresponding to each representative day, according to data from the year 2020, can be seen in Fig. 8, showing the average direct normal irradiance (DNI) for each month of the year over a one-day period. This analysis is important for developing the calculations set out above. The normal direct irradiance of João Pessoa for each typical day chosen shows variations throughout the 24 hours analysed depending on meteorological factors, such as cloudiness and rain. The hottest months in João Pessoa are from November to March. However, the graph for 2020 showed atypical behaviour for December and February. June is the coldest month.

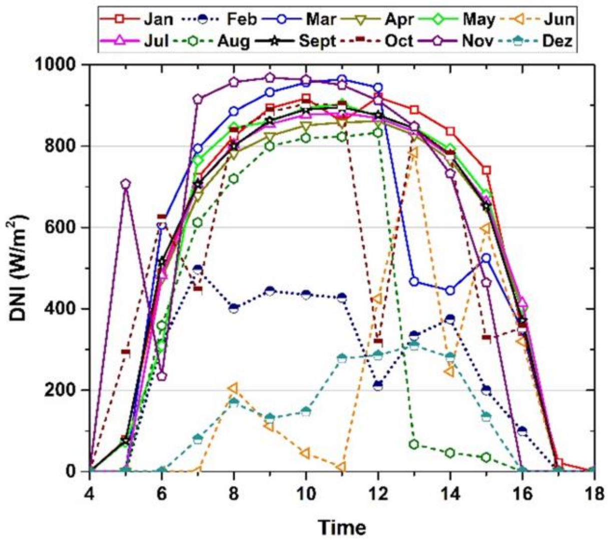

Fig. 8. Average DNI for each month of the year.

3. Results and discussion

3.1. Validation of the ORC with benchmark

Table 4 presents the verified efficiency results of the organic Rankine cycle and the global efficiency of the solar cycle for different collectors and fluids. The calculated results of the present study are quite satisfactory and show good agreement with the reference work by Delgado-Torres and García-Rodríguez [5] used for validation, with percentage errors of less than 5%.

3.2. Cycle with parabolic trough collector

Figure 9 shows the energetic and exergetic efficiency of the organic Rankine cycle for the parabolic trough collector (PTC) collector. This collector presented a greater range of use of organic fluids for the solar organic Rankine cycle, as it obtained the best overall system efficiency, in addition to the smaller opening areas required for installation. This is justified by the fact that the average operating temperature range is greater than that of other collectors, which makes it possible to obtain greater applicability for different fluids.

Table 4. Validation of the results of the present study with the reference work.

Cycle Parameters					Organic Rankine Cycle Efficiency			Solar Power Cycle Efficiency		
Collector	Fluid	P_{cond} (kPa)	P_{evap} (kPa)	T_2 (°C)	η_{ORC} (%) Reference	η_{ORC} (%) Present Study	Error (%)	η (%) Reference	η (%) Present Study	Error (%)
Aosol 1.12 X (CPC)	Isobutane	404.7	1400	95	9.95	9.86	0.90	3.91	3.98	1.79
	Isopentane	109.2	491.6	95	10.49	10.51	0.19	4.03	4.11	1.99
	R245fa	177.8	829.6	95	10.14	10.15	0.10	3.97	4.04	1.76
VITOSOL 200F (FPC)	Isobutane	404.7	1371	95	9.85	9.96	1.12	4.32	4.40	1.85
	Isopentane	109.2	491.6	95	10.49	10.51	0.19	4.45	4.54	2.02
	R245fa	177.8	829.6	95	10.14	10.15	0.10	4.39	4.47	1.82
VITOSOL 300 (Evacuated)	Isobutane	404.7	2395	145	14.94	14.41	3.55	8.11	7.96	1.85
	Isopentane	109.2	1288	145	16.40	16.48	0.49	8.51	8.78	3.17
	R245fa	177.8	2087	145	15.46	15.48	0.13	8.26	8.44	2.18

As shown in Fig. 9, the toluene fluid, which is a dry fluid, presents the highest efficiencies with the variation of evaporation pressure. This is related to the fluid saturation curve, in which the toluene saturation temperature is greater than that of other fluids analysed for the same simulated evaporation pressure. As can be seen, the cycle using toluene fluid at a pressure of 2500 kPa achieves 21.62% thermal efficiency and 23.61% exergy efficiency.

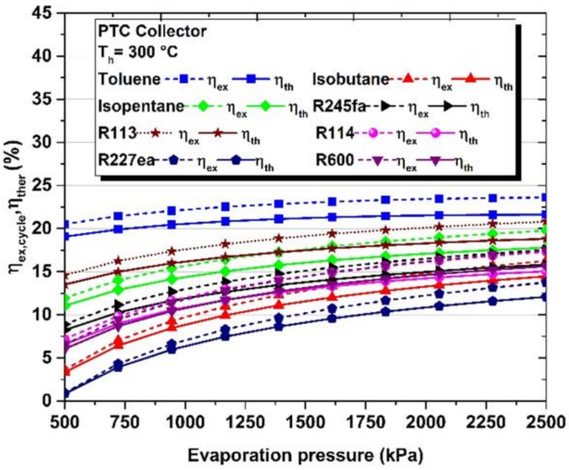

Fig. 9. Exergy and energy efficiency as a function of evaporation pressure for the PTC collector.

Figure 10 shows the variation in the mass flow in relation to the evaporation pressure. It can be noted that there is an inversely proportional relationship between these two variables, in which the circulating flow of fluid in the system decreases as the pressure increases. Toluene and isopentane were the fluids that presented the lowest mass flow values within the pressure range chosen for the simulation, in which the mass flow values did not exhibit significant variations. Furthermore, at higher pressures, the mass flow values did not vary significantly, remaining almost constant. Mass flow rates are directly related to the system size and required pumping power.

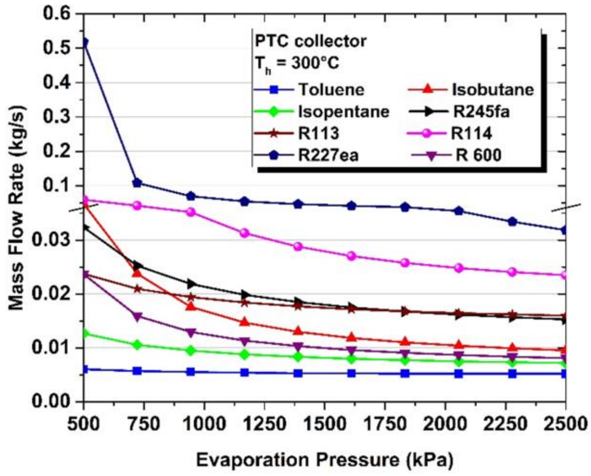

Fig. 10. Mass flow rate as a function of evaporation pressure for the PTC collector.

Figure 11 shows the variation in the opening area in relation to the evaporation pressure. The opening area decreases with the increasing evaporation pressure. R227ea fluid at 50 kPa pressure requires 117.8 m^2 and at 250 kPa pressure requires 8.3 m^2. Furthermore, a relationship can be seen in which not necessarily increasing the collector area will increase the cycle efficiency. In general, among the fluids analysed, the area values did not show sudden changes beyond a pressure of 1500 kPa. Toluene, R113 and isopentane fluids require smaller areas to install a solar plant of this model.

Figure 12 presents the exergy efficiency analysis of the turbine as a function of the evaporation pressure. For different fluid flow rates, the change in turbine exergy destruction depends on the evaporator pressure. If R227ea is chosen as the refrigerant, the exergy efficiency of the turbine is maximum, and the exergy efficiency increases from 84.27% to 85.18%. However, if toluene is used, the exergy efficiency increases from 80.71% to 82.45%.

Figure 13 shows the exergy efficiency of the condenser as a function of the evaporation pressure. When R227ea is used as

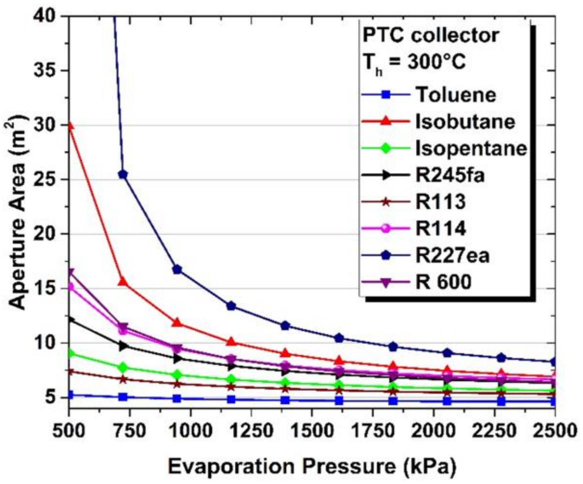

Fig. 11. PTC collector aperture area as a function of evaporation pressure.

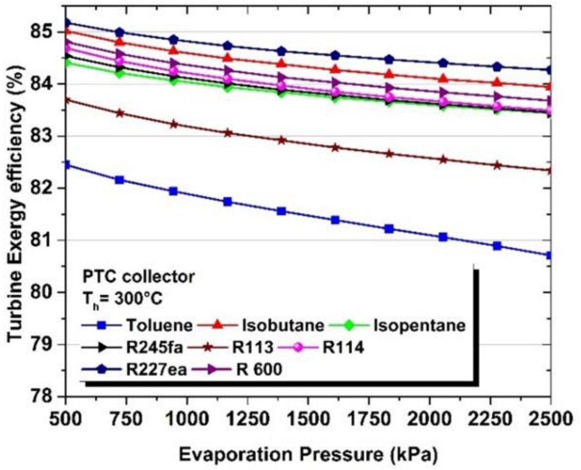

Fig. 12. Turbine exergy efficiency as a function of evaporation pressure.

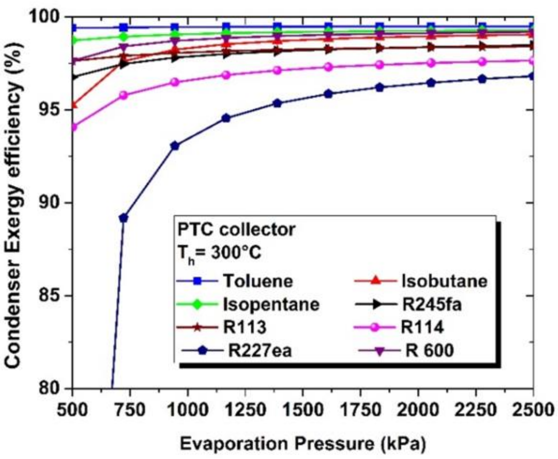

Fig. 13. Condenser exergy efficiency as a function of evaporation pressure.

a refrigerant, depending on the evaporator pressure, the maximum variation in the exergy efficiency of the condenser is approximately 50.27%, ranging from 48.14% to 96.81%. However, if toluene is preferred, the variation in the condenser exergy efficiency is minimal and approximately 0.08%, ranging from 99.4% to 99.48%. For the different refrigerants, the changes in the regenerator exergy efficiency are shown in Fig. 14. When R227ea is used, the change in the exergy efficiency of the heat exchanger is maximum depending on the evaporator pressure, ranging from 25.44% to 52.85%. However, if toluene is chosen as the refrigerant, the change in the exergy efficiency of the heat exchanger is minimal at 1.18%.

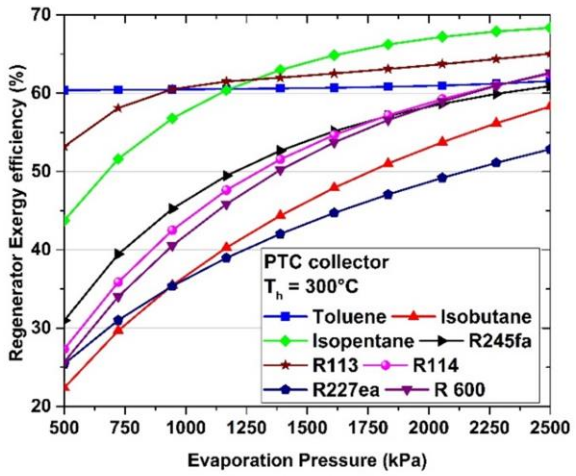

Fig. 14. Regenerator exergy efficiency as a function of evaporation pressure.

Figure 15 shows the exergy efficiency of the evaporator as a function of the evaporation pressure. When R227 and R114 are used as refrigerants, the evaporator exergy efficiency is maximum and reaches up to 30% depending on the evaporator pressure.

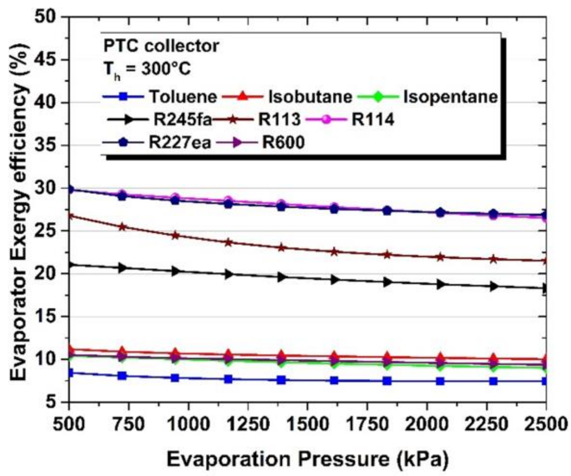

Fig. 15. Evaporator exergy efficiency as a function of evaporation pressure.

3.3. Cycle with compound parabolic collector

Figures 16 and 17 show the resulting performance parameters and the variation in the mass flow for the compound parabolic collector (CPC) as a function of the evaporation pressure, respectively. For application in CPCs, the thermodynamic analysis showed an unfeasibility entropy generation for the toluene fluid within the recommended temperature operating range of the solar concentrator, a factor consistent with works found in current literature, in which there is the possibility of using isobutane and R245fa in these lower temperature ranges, in which they are common in geothermal applications [13]. As can be seen, using CPC collector in the cycle depending on the fluid only achieves 1.83% thermal efficiency and 2.02% exergy efficiency.

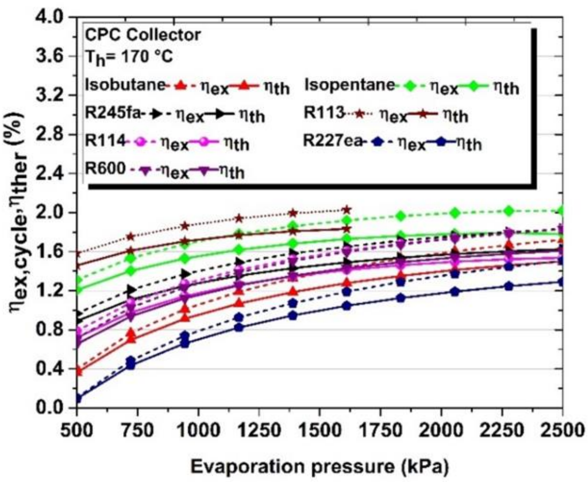

Fig. 16. Exergy and energy efficiency as a function of evaporation pressure for the CPC collector.

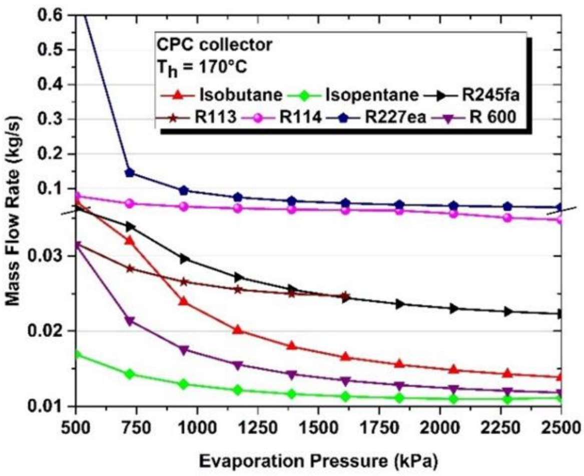

Fig. 17. Mass flow rate as a function of evaporation pressure for the CPC collector.

The efficiencies of the plant with the CPC concentrator for all fluids used in the simulation are very low. In addition, the areas calculated with these fluids (Fig. 18) make applications related to power plants with solar energy unfeasible from a practical point of view.

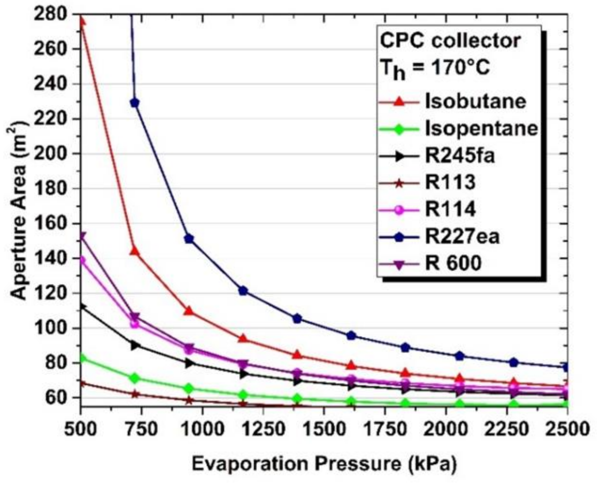

Fig. 18. CPC collector aperture area as a function of evaporation pressure.

It can be highlighted that for R600, the presence of a minimum area of 60 m² with low flow provides a maximum efficiency of 1.8% for this working fluid, and this should be the operating point selected in the case of using this working fluid coupled to CPC. Therefore, it is recommended to use another type of collector with higher temperatures, such as PTC, as it makes more sense to obtain greater efficiency and a smaller opening area.

3.4. Case study (João Pessoa, Brazil)

The effect of solar radiation and ambient temperature on the system performance in a city is evaluated in this section. The city of João Pessoa, in eastern Brazil, has impressive solar potential due to the abundance of solar radiation throughout the year. Therefore, it was chosen as an option for implementing the studied system.

Figures 19 and 20 demonstrate how solar irradiation and ambient temperature affect exergy and thermal efficiency, respec-

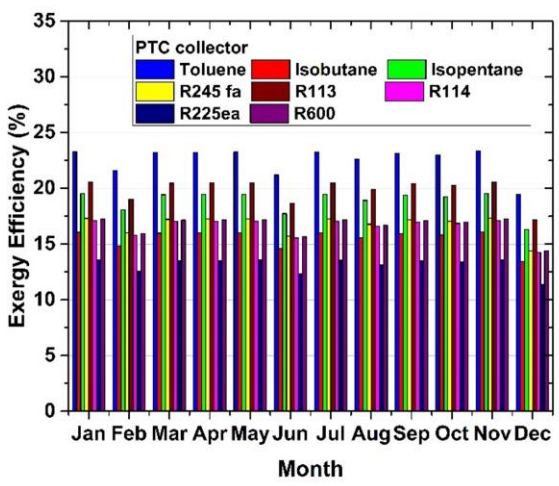

Fig. 19. System exergy efficiency with PTC collector for the year 2020 in the city of João Pessoa, Brazil.

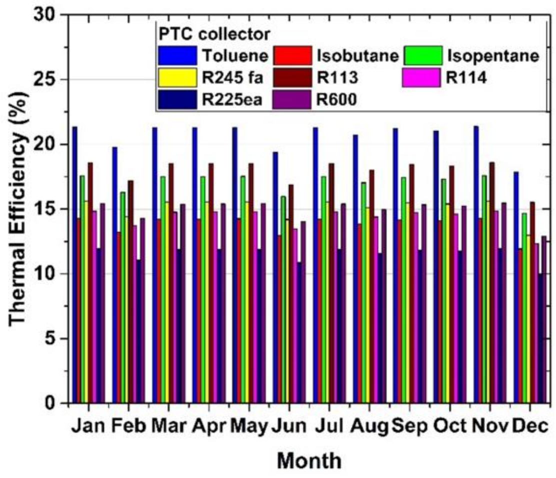

Fig. 20. System thermal efficiency with PTC collector for the year 2020 in the city of João Pessoa, Brazil.

tively. According to Fig. 19, the greatest exergy efficiency occurs in the months of January (21.37%), March (21.26%) and November (21.35%) − the hottest months of the year, when the sun shines intensely. Based on Fig. 8, the greater the solar irradiation, the greater the exergy and thermal efficiency. Unlike solar intensity, which positively affects exergy efficiency, an increase of the ambient temperature decreases exergy and thermal efficiency. Therefore, its lowest value occurs in June. December's results are atypical for the year 2020.

4. Conclusions

In this study, cycle energy and exergy analyses based on the evaporator pressure change were performed for a power generation plant using solar energy with different refrigerants. It can be concluded that:

- With the adequate selection of the refrigerant, collector, and evaporation pressure, the first and second law efficiencies of the cycle improve up to 41% and 44%, respectively.
- The best use of incident solar radiation occurred with the fluid toluene among the refrigerants used, due to the high thermal and exergy efficiency of the cycle, and presented the smallest opening area (4.6 m^2) required per unit kW, indicating that its adoption would result in a more compact solar field, while R227ea presented the lower thermal and exergy performance than other refrigerants.
- The parabolic trough collector achieved the best results from the point of view of energy (21.62%) and exergy (23.62%) efficiency, due to obtaining high temperatures, which resulted in the optimum concentration efficiency.
- The thermodynamic analysis of the compound parabolic collector showed an unfeasible entropy generation in the heat exchangers for isopentane and toluene, indicating the impossibility of using these working fluids within the selected pressure range at the maximum temperatures reached by this type of collector. The use of a compound parabolic collector in the cycle depending on the fluid achieves only 1.83% thermal efficiency and 2.02% exergy efficiency.
- Depending on the refrigerant and evaporator pressure, the exergy efficiency of the turbine reaches 86.22%, while that of the evaporator reaches 76.6%.
- For the city of João Pessoa, the highest exergy efficiency occurs in the months of January (21.37%) and November (21.35%), the hottest months of the year, when the sun shines brightly, and the lowest exergy efficiency occurs in the month of June (19.41%).

Finally, this study on the organic Rankine cycle with solar concentrators can assist research and development projects in the dissemination and maturation of the topic in the national territory, being another option to be analysed from an economic and environmental point of view for its more significant insertion in the Brazilian electrical matrix.

Acknowledgements

The first author thanks for the support of the Paraiba State Research Foundation − FAPESQ Brazil (Term no. 066/2023, Edict no. 19-2022).

References

[1] Colonna, P., Casati, E., Trapp, C., Mathijssen, T., Larjola, J., Turunen-Saaresti, T., & Uusitalo, A. (2015). Organic Rankine cycle power systems: From the concept to current technology, applications, and an outlook to the future. *Journal of Engineering for Gas Turbines and Powe*r, 137(1), 1−19. doi: 10.1115/1.4029884

[2] Loni, R., Mahian, O.M., Markides, C.N., Bellos, E., Roux, W.G.L, Kasaeian, A., Najafi, G., & Rajaee, F. (2021). A review of solar-driven organic Rankine cycles: recent challenges and future outlook. *Renewable and Sustainable Energy Reviews*, 150, 111410. doi: 10.1016/j.rser.2021.111410

[3] Petrollese, M.; Cau, G., & Cocco, D. (2020). The Ottana solar facility: dispatchable power from small-scale CSP plants based on ORC systems. *Renewable Energy*, 147, 2932−2943. doi: 10.1016/j.renene.2018.07.013

[4] Ancona, M.A. Bianchi, M., Branchini, L., De Pascale, A., Melino, F., Peretto, A., Poletto, C., & Torricelli, N. (2022). Solar driven micro-ORC system assessment for residential application. *Renewable Energy*, 195, 167−181. doi: 10.1016/ j.renene.2022.06.007

[5] Delgado-Torres, A.M., & García-Rodríguez, L. (2010). Analysis and optimization of the low-temperature solar organic Rankine cycle (ORC). *Energy Conversion and Management*, 51(12), 2846−2856. doi: 10.1016/j.enconman.2010.06.022

[6] Jing, L., Gang, P., & Jie, J. (2010). Optimization of low temperature solar thermal electric generation with Organic Rankine Cycle in different areas. *Applied Energy*, 87(11), 3355–3365. doi: 10.1016/j.apenergy.2010.05.013

[7] Kumar, A., & Shukla, S.K. (2016). Analysis and performance of ORC based solar thermal power plant using benzene as a working fluid. *Procedia Technology*, 23, 454−463. doi: 10.1016/j.protcy.2016.03.050

[8] Sonsaree, S., Asaoka, T., Jiajitsawat, S., Aguirre, H., & Tanaka, K. (2018). A small-scale solar organic Rankine cycle power plant in Thailand: Three types of non-concentrating solar collectors, *Solar Energy*, 162, 541–560. doi: 10.1016/j.solener.2018.01.038

[9] Stand, L.M., Ochoa, G.V., & Forero, J.D. (2021). Energy and exergy assessment of a combined supercritical Brayton cycle −

ORC hybrid system using solar radiation and coconut shell biomass as energy source. *Renewable Energy*, 175, 119−142. doi: 10.1016/j.renene.2021.04.118

[10] Gupta, P.R., Tiwari, A.K., & Said, Z. (2022). Solar organic Rankine cycle and its poly-generation applications – A review. *Sustainable Energy Technologies and Assessments*, 49, 101732. doi: 10.1016/j.seta.2021.101732

[11] Lakhani, S.; Raul, A., & Saha, S.K. (2017). Dynamic modelling of ORC-based solar thermal power plant integrated with multitube shell and tube latent heat thermal storage system. *Applied Thermal Engineering*, 123, 458−470. doi: 10.1016/j.applthermaleng.2017.05.115

[12] Li, J.F., Guo, H., Wu, Y.T., Lei, B., Ye, F., Ma, C.F., Zhang, Y., & Jiao, X.L. (2022). Experimental investigation of solar organic Rankine cycle with parabolic trough concentrator using nitrate salt as heat transfer and storage fluid, *International Journal of Energy Research*, 46, 6847−6865. doi: 10.1002/er.7628

[13] Ahmadi, A., El Haj Assad, M., Jamali, D.H., Kumar, R., Li, Z.X., Salameh, T., Al-Shabi, M., & Ehyaei, M.A. (2020). Applications of geothermal organic Rankine Cycle for electricity production. *Journal of Cleaner Production*, 274, 122950. doi: 10.1016/j.jclepro.2020.122950

[14] Saadatfar, B., Fakhrai, R., & Fransson, T. (2014). Conceptual modeling of nano fluid ORC for solar thermal polygeneration. *Energy Procedia*, 57, 2696−2705. doi: 10.1016/j.egypro.2014.10.301

[15] Rejeb, O., Alirahmi, S.M., Assareh, E., El Haj Assad, M., Jemni, A., Bettayeb, M., & Ghenai, C. (2022). Innovative integrated solar powered polygeneration system for green hydrogen, oxygen, electricity and heat production. *Energy Conversion and Management*, 269, 116073. doi: 10.1016/j.enconman.2022.116073

[16] Jiang, Y., Zhang, X., Zhang, Z., Hao, L., Cao, Z., Li, S., Guo, B., Zheng, Y., Dong, C., & Zhao, L. (2024). Performance evaluation and working fluid screening of direct vapor generation for solar ORC using low-global warming potential (GWP) working fluids. *Energies*, 17, 3133. doi: 10.3390/en17133133

[17] Maytorena, V.M., & Buentello-Montoya, D.A. (2022). Multiphase simulation and parametric study of direct vapor generation for a solar organic Rankine cycle. *Applied Thermal Engineering*, 216, 119096. doi: 10.1016/j.applthermaleng.2022.119096

[18] Hepbasli, A. (2008). A key review on exergetic analysis and assessment of renewable energy resources for a sustainable future. *Renewable and Sustainable Energy Reviews*, 12(3), 593−661. doi: 10.1016/j.rser.2006.10.001

[19] Nafey, A.S., & Sharaf, M.A. (2010). Combined solar organic Rankine cycle with reverse osmosis desalination process: Energy, exergy, and cost evaluations. *Renewable Energy*, 35(11), 2571−2580. doi: 10.1016/j.renene.2010.03.034

[20] Kalogirou, A.S. (2013). *Solar Energy Engineering: Process and Systems*. Academic Press.

[21] Klein, S.A. (1977). Calculation of monthly average insolation on tilted surfaces. *Solar Energy*, 19(4), 325−329. doi: 10.1016/0038-092X(77)90001-9